Structure and Mechanical Properties of Mesostructured Functional Hybrid Coatings Based on Anisotropic Nanoparticles Dispersed in Poly(hydroxylethyl methacrylate)

Nicolas Chemin,[†,‡,§,⊥] Laurence Rozes,[†,‡] Corinne Chanéac,[†,‡] Sophie Cassaignon,[†,‡] Eric Le Bourhis,[§] Jean-Pierre Jolivet,[†,‡] Olivier Spalla,[||] Etienne Barthel,[⊥] and Clément Sanchez*[,†,‡]

UPMC Univ Paris 06, UMR 7574, LCMCP, 4 place Jussieu, case 174, F-75005, Paris, France, CNRS, UMR 7574, LCMCP, F-75005, Paris, France, Laboratoire de Physique des Matériaux, UMR 6630 CNRS, Université de Poitiers, SP2MI, Boulevard Marie et Pierre Curie, F-86962, Futuroscope Chasseneuil cedex, France, CEA Saclay, IRAMIS/SCM, LIONS, F-91191, Gif sur Yvette, France, and Surface du Verre et Interfaces, CNRS/Saint-Gobain, UMR 125, 39 quai Lucien Lefranc, F-93303, Aubervilliers, France

Received January 25, 2008. Revised Manuscript Received March 26, 2008

Colored hybrid coatings with efficient mechanical properties have been elaborated by introducing goethite (α-FeOOH) nanorods and maghemite (γ-Fe_2O_3) nanospheres in a poly(hydroxyethyl methacrylate) (PHEMA) matrix. The resulting hybrid coatings have been characterized with regard to the dispersion state of the particles, the swelling behavior of the PHEMA matrix, and the mechanical properties of the coatings. From a mechanical point of view, both goethite nanorods and maghemite nanospheres lead to a strong reinforcement effect of PHEMA, even at low volume fraction. The origin of such reinforcement is attributed to the existence of strong interactions at the iron oxide–PHEMA interface combined with a homogeneous dispersion of the particles. The nature and the strength of these interactions and evidence of their influence on the mechanical behavior of the nanohybrid coatings are reported. Moreover, the goethite-based hybrid coatings exhibit interesting birefringent properties associated with the stabilization inside the organic matrix of a liquid crystal-type organization resulting from the self-assembly of goethite nanorods.

Introduction

Organic−inorganic hybrid materials do not only represent a creative alternative to design new materials and compounds for academic research, but their improved or unusual features allow one to develop innovative industrial applications.[1] Hybrid materials[2,3] are not simply physical mixtures, but they can be broadly defined as nanocomposites with organic and inorganic components intimately mixed at the nanoscopic level.[4–7] Obviously, the properties of the final materials are not only the sum of the primary components, and a large synergy effect is expected from the close coexistence of the two phases through size domain effects and the nature of the interfaces.

The introduction of fillers in polymer matrices meets a well-established industrial scheme that aims at enhancing specific properties of polymers while reducing production costs. Composite structures provide an efficient method to produce easily processed and stable materials with interesting optical, electrical, thermal, magnetic, or mechanical properties.[8,9] The choice of polymer component, which is generally guided by their mechanical and thermal behavior, can also provide biocompatibility, optical and electronic properties, and wettability. However, in many cases, the polymeric organic components also allow an easy shaping and a better processing of the composite materials. The inorganic components can provide mechanical and thermal stability, fireproof enhancements, but also new functionalities that depend on the chemical nature, structure, size, and crystallinity of the inorganic filler phase.[5,10] Indeed, the inorganic component can implement or improve electronic and magnetic properties, barrier properties, density, refraction index, coloration,[8] etc.

An important category of hybrid materials that shows promising industrial developments concerns hybrid nanocomposites where a polymer matrix is filled by functional nano-objects. The properties of nanophase materials depend

* Corresponding author. Tel.: (33)-1-44 27 55 34. Fax: (33)-1-44 27 47 69. E-mail: clement.sanchez@upmc.fr.
† UPMC Univ Paris 06.
‡ CNRS.
§ Université de Poitiers.
⊥ CNRS/Saint-Gobain.
|| CEA Saclay.

(1) Sanchez, C.; Julián, B.; Belleville, P.; Popall, M. *J. Mater. Chem.* **2005**, *15*, 3559.
(2) Sanchez, C.; Ribot, F. *New J. Chem.* **1994**, *18*, 1007.
(3) Sanchez, C.; Soler-Illia, G. J. de A. A.; Ribot, F.; Lalot, T.; Mayer, C. R.; Cabuil, V. *Chem. Mater.* **2001**, *13*, 3061.
(4) Giannelis, P. *Adv. Mater.* **1996**, *8*, 29.
(5) *Hybrid Materials, Synthesis, Characterization, and Applications*; Kickelbick, G., Ed.; Wiley: New York, 2007.
(6) Alexander, M.; Dubois, P. *Mater. Sci. Eng.* **2000**, *28*, 1.
(7) Ray, S.; Okamoto, M. *Prog. Polym. Sci.* **2003**, *28*, 1539.
(8) *Functional Hybrid Materials*; Gomez, R., Sanchez, C., Eds.; Wiley: New York, 2004.
(9) Mammeri, F.; Le Bourhis, E.; Rozes, L.; Sanchez, C. *J. Mater. Chem.* **2005**, *15*, 3787.
(10) Kickelbick, G. *Prog. Polym. Sci.* **2003**, *28*, 83.

10.1021/cm800253s CCC: $40.75
Published on Web 06/18/2008

not only on the individual properties of the components but also on their organization throughout the composite as well as their interfacial characteristics. When nanoparticles are homogeneously dispersed in polymer matrices, the resulting nanomaterials benefit from the specific characteristics of the fillers. Moreover, some value-added properties can make a big difference in terms of applications and marketing. For example, in contrast to conventional filled composites, which are opaque, low volume-fraction additions and nanoscopic dimensions of the well-dispersed nanofillers result in hybrid nanocomposites with optical transparency, comparable to the base polymeric matrix.

Pioneering work of Toyota researchers on clay nanocomposites[11–14] as well as recent breakthroughs in carbon nanotube technologies[15,16] have spurred new endeavors to incorporate nanofillers in organic matrices. Particularly, oxide nanoparticles have emerged as an interesting route to confer novel functionalities to materials while strengthening them mechanically.[17–24] For instance, cerium oxide and silica nanoparticles were used in antireflective coating to tune the refractive index and improve the abrasion resistance.[24] Similarly, incorporation of ZnO particles in vinylester resin results in nanocomposites with enhanced photoluminescence properties and significant tensile strength improvement.[20]

The colors and magnetic properties of iron oxides make them of particular interest to elaborate functional nanocomposites. The structural chemistry of iron oxi(hydroxi)des is very rich and diversified since more than a dozen structural types have been identified[25] and almost all of them can be formed from solution by "Chimie Douce",[26] which allows for precise control over size and shape. However, only a few research works describe their incorporation into polymer matrices.[16,18,27–31] Moreover, the structure and the resulting mechanical properties of iron oxide-based hybrid nanocomposites have not been studied extensively.

In the present work, we report the synthesis and the structural and mechanical characterization by nanoindentation of organic−inorganic hybrid coatings based on poly(2-hydroxyethyl methacrylate) (PHEMA) and anisotropic rod-shaped goethite nanoparticles. Isotropic spherical maghemite nanoparticles were also used as nanofillers to determine the influence of the particles' aspect ratio. Particular emphasis is given to the investigation of the role of the interface bonding, the filler content, the filler dispersion, and the filler aspect ratio on their mechanical properties. Moreover, these hybrids exhibit birefringent properties associated with the stabilization inside the organic matrix of a liquid crystalline organization resulting from the self-assembly of goethite nanorods.

In this work, specific film ellipsometry measurements were used to determine the amount of swelling in the films. In addition, small-angle X-ray scattering (SAXS) and transmission electronic microscopy (TEM) were developed to investigate the dispersion and the orientation of the filler in the polymer matrix. In addition, the bounding mode between PHEMA and the iron oxide surface was examined by Fourier transform infrared spectroscopy (FTIR) on HEMA-capped iron oxide nanoparticles.

Experimental Section

Preparation of Iron Oxide Nanoparticles. Stable aqueous suspensions of non aggregated goethite and maghemite nanoparticles were prepared. Goethite (α-FeOOH) nanorods were synthesized by hydrolysis of ferric ions by addition of base in solution at room temperature as described elsewhere.[26,32] After an aqueous solution of $Fe(NO_3)_3$ (400 mL, 0.1 M) was aged at pH = 11 for 15 days, rod-shaped nanoparticles were obtained with average length of 300 nm, width of 30 nm, and thickness of 10 nm. Maghemite nanoparticles exhibiting a spherical shape of 8 nm in diameter were prepared according to literature procedure.[33] Spinel iron oxide Fe_3O_4 was first precipitated by addition of ferrous and ferric ions (Fe(II)/Fe(III) = 0.5); iron treatment using perchloric acid solution (3 M) has been used to obtain fully oxidized spinel iron oxide, γ-Fe_20_3.[26]

Preparation of PHEMA–Iron Oxide Nanocomposites. The elaboration of the nanohybrid coatings was conducted by in situ UV polymerization of the HEMA monomer in the presence of rod-shaped goethite nanoparticles or spherical maghemite nanoparticles with different volume fractions. The aqueous nanoparticle sols were directly introduced in the HEMA monomer. After addition of 2 wt % of a photoinitiator (2,2-dimethoxy-2-phenylacetophenone from Aldrich), homogeneous solutions were obtained and stirred for 48−96 h at room temperature before deposition.

Films were spin-coated from the hybrid solutions on standard float glass (Saint-Gobain, France), silicon wafers, as well as 150 μm thick glass substrates and polymerized under UV light (365 nm, 2 × 6 W) during 1 h. 50 mm × 25 mm standard size substrates have been coated. Nevertheless, the size of the coating is not limited.

(11) Usuki, A.; Kojima, M.; Okada, A.; Fukishima, Y.; Kurauchi, T.; Kamigaito, O. *J. Mater. Res.* **1993**, *8*, 1179.
(12) Usuki, A.; Kojima, M.; Kawasumi, M.; Okada, A.; Fukishima, Y.; Kurauchi, T.; Kamigaito, O. *J. Mater. Res.* **1993**, *8*, 1185.
(13) Russo, G. M.; Simon, G. P.; Incarnato, L. *Macromolecules* **2006**, *39*, 3855.
(14) Rao, Y.; Pochan, J. M. *Macromolecules* **2007**, *40*, 290.
(15) Liu, T.; Phang, I. Y.; Shen, L.; Chow, S. Y.; Zhang, W.-D. *Macromolecules* **2004**, *37*, 7214.
(16) Olek, M.; Kempa, K.; Jurga, S.; Giersig, M. *Langmuir* **2005**, *21*, 3146.
(17) Ash, B. J.; Siegel, R. W.; Schadler, L. S. *Macromolecules* **2004**, *37*, 1358.
(18) Ciprari, D.; Jacob, K.; Tannenbaum, R. *Macromolecules* **2006**, *39*, 6565.
(19) Gass, J.; Poddar, P.; Almand, J.; Srinath, S.; Srikanth, H. *Adv. Funct. Mater.* **2006**, *16*, 71.
(20) Guo, Z.; Wei, S.; Shedd, B.; Scaffaro, R.; Pereira, T.; Hahn, H. T. *J. Mater. Chem.* **2006**, 806.
(21) Guo, Z.; Wei, S.; Pereira, T.; Choi, O.; Wang, Y.; Hahn, H. T. *J. Mater. Chem.* **2006**, 2800.
(22) Ji, X.; Hampsey, J. E.; Hu, Q.; He, J.; Yang, Z.; Lu, Y. *Chem. Mater.* **2003**, *15*, 3656.
(23) Khaled, S. M.; Sui, R.; Charpentier, P. A.; Rizkalla, A. *Langmuir* **2007**, *23*, 3988.
(24) Krogman, K. C.; Druffel, T.; Sunkara, M. K. *Nanotechnology* **2005**, *16*, S338.
(25) Cornell, R. M.; Schertmann, U. *The Iron Oxides: Structure, Properties, Reactions, Occurrence and Uses*; VCH Publishers: Weinheim, 1996.
(26) Jolivet, J. P.; Tronc, E.; Chanéac, C. *Chem. Commun.* **2004**, 481.
(27) Tannenbaum, R.; Zubris, M.; Goldberg, E. P.; Reich, S.; Dan, N. *Macromolecules* **2005**, *38*, 4254.
(28) Dallas, P.; Georgakilas, V.; Niarchos, D. *Nanotechnology* **2006**, *17*, 2046.
(29) Baker, C.; Ismat Shah, S.; Hasanain, S. K. *J. Magn. Magn. Mater.* **2004**, *280*, 412.
(30) Lopez, D.; Cendoya, I.; Torres, F.; Tejada, J.; Mijangos, C. *J. Appl. Polym. Sci.* **2001**, 3215.
(31) Aoyama, S.; Kishimoto, M.; Manabe, T. *J. Mater. Chem.* **1992**, *2*, 277.
(32) Atkinson, R. J.; Posner, A. M.; Quirk, J. P. *J. Phys. Chem.* **1967**, *71*, 550.
(33) Vayssières, L.; Chanéac, C.; Tronc, E.; Jolivet, J. P. *J. Colloid Interface Sci.* **1998**, *205*, 205.

Bulk materials were also produced by casting the hybrid solutions in Teflon molds. Note that a longer polymerization time (depending on the thickness) was required for the bulk material.

At the end of the polymerization step, the films and the bulk nanocomposites underwent a final thermal treatment at 120 °C for 24 h to ensure a good monomer conversion.

Characterization of PHEMA–Iron Oxide Nanocomposites. (i) The content of the inorganic phase in the nanocomposites was determined by thermogravimetric analysis (TGA) and elemental analysis. Thermogravimetric analysis (Perkin-Elmer) was conducted from 25 to 600 °C with an air flow rate of 50 cm^3 min^{-1} and a heating rate of 10 °C min^{-1}.

(ii) The homogeneity of the dispersion of the nanorods in the matrix was evaluated by transmission electron microscopy (TEM) on the PHEMA–iron oxide nanocomposites using a Philips CM20/STEM transmission electron microscope at a voltage of 200 kV. The samples were prepared from scrapped hybrid coatings embedded in an epoxy resin and microtomed into electron beam transparent films. Scanning electron microscopy (SEM) with a field gun (ZEIS Gemini DSM 982) operated at a voltage of 5 kV was used to further investigate the dispersion state of the particles in depth of the coating.

(iii) Small-angle X-ray scattering (SAXS) measurements were carried out on PHEMA–goethite nanocomposites. Because of the size of the goethite particle, a complementary set of two SAXS experiments was used to measure the intensities scattered by such materials. A first SAXS camera makes it possible to measure in the q-range 2×10^{-2} to 0.4 $Å^{-1}$,[34] which is sensitive to the small length scales. The second setup was a USAXS camera[35] with an observation range going from 3×10^{-4} to 0.1 $Å^{-1}$, which is more adapted to the larger dimension of the goethite nanorods. Measurements were performed both on powder from scrapped hybrid coatings and directly on the hybrid coatings deposited on a 150 μm thick glass substrate. The measured scattering diagram $I(q)$ for each specimen has been corrected for the background and the smearing effects. A further subtraction of the PHEMA profile was performed to obtain the scattered intensity from the goethite nanorods alone. As compared to SAXS measurements performed on powdered bulk nanocomposites, which can be affected (particularly in the USAXS range) by powder grain scattering, SAXS transmission measurements performed on hybrid coatings deposited on 150 μm thick glass substrate revealed to be an efficient method to investigate the dispersion of the goethite nanoparticles in the PHEMA matrix. Despite glass absorption and coating thinness, SAXS profiles have been recorded in good conditions.

Characterization of the PHEMA–Iron Oxide Interface. (i) The minimum amount of material available in a film severely limits the range of structural characterization. The strength of interaction between goethite nanoparticles and the PHEMA matrix for increasing goethite content was first studied using equilibrium swelling measurements on the bulk hybrid materials. Pieces of each sample were cut and put into THF. After 72 h at room temperature, the samples were taken out of the liquid, and solvent was removed from the surface, to determine the weight of the swollen samples. The swelling ratio (SR) is calculated as follows:

$$\mathrm{SR} = \frac{W_s - W_{ums}}{W_{ums}} \times 100 \qquad (1)$$

where W_s is the weight of the swollen sample and W_{uns} is the weight of the dry sample.

If the characterization of bulk materials may be considered a good alternative to obtain a rough estimate of film properties, it is always difficult to extrapolate the characteristics of the bulk to that of the coating. Because specific film properties may arise from deposition method induced by substrate, preferential orientation, or thickness effects, a characterization of the swelling behavior of the hybrid coatings was carried out also by ellipsometry. Ellipsometry measurements were performed using a variable angle spectroscopic ellipsometer (EquipmentWoollamM2000U) equipped with a humidity-controlled chamber. The thickness and the refractive index of the hybrid coatings prepared onto Si substrates were measured as a function of the relative humidity. The wavelength range chosen for this study was 500−800 nm, where iron oxide nanoparticles are nonabsorbing.[25] When relative humidity was incremented in the cell, measurements were not performed until relative humidity stabilization that usually required 4−5 min. After this time, the coating thickness had already reached equilibrium value, indicating fast swelling kinetics.

(ii) To study the adsorption of the HEMA monomer at the goethite surface, the hybrid solutions of goethite nanoparticles in HEMA were centrifuged before polymerization. The unadsorbed monomer was removed with the supernatant; the particles were washed twice with deionized water and dried under nitrogen. Adsorption study of HEMA at goethite surface was investigated using Fourier transform infrared (FT-IR) spectroscopy using an FTIR spectrometer (Nicolet) in transmission. Attenuated total reflection (ATR) infrared spectroscopy was applied to record the spectrum of pure HEMA as a reference to be compared to the spectrum of HEMA-coated goethite nanoparticles recorded in KBr at a resolution of 4 cm^{-1} and 32 scans.

Characterization of the Film Mechanical Properties. Nanoindentation-based techniques have proved to be powerful tools that can provide quantitative information regarding the mechanical properties of hybrid coatings.[36–40] Nanoindentation tests were investigated by using an instrumented nanoindenter XP (MTS) with a Berkovich tip. The force, penetration, and contact stiffness at 45 Hz during 250 nm deep indentation runs were recorded and converted to elastic modulus and hardness by the Oliver and Pharr[41] method. Note that nanoindentation measurements allow the direct determination of the reduced elastic modulus E_r of the film. The elastic modulus of the film E was calculated from the reduced elastic modulus using the expression:

$$E_r = \frac{E}{1 - \nu^2} \qquad (2)$$

where ν is Poisson's ratio for the tested material (taken as 0.3).

Results and Discussion

The high degree of solubility in water of HEMA ($C_W = \infty$)[42] allows the direct introduction of iron oxide aqueous suspensions without further surface modification of the nanoparticles. During stirring at room temperature, the viscosity of the hybrid HEMA–iron oxide solutions increases,

(34) Zemb, T.; Tache, O.; Ne, F.; Spalla, O. *J. Appl. Crystallogr.* **2003**, *36*, 800.
(35) Lambard, J.; Lesieur, P.; Zemb, T. *J. Phys. I* **1992**, *2*, 1191.
(36) Mammeri, F.; Le Bourhis, E.; Rozes, L.; Sanchez, C. *J. Non-Cryst. Solids* **2004**, *345*, 346–610.
(37) Mammeri, F.; Rozes, L.; Le Bourhis, E.; Sanchez, C. *J. Sol.-Gel Sci. Technol.* **2003**, *26*, 413.
(38) Douce, J.; Boilot, J.-P.; Biteau, J.; Scodellaro, L.; Jimenez, A. *Thin Solid Films* **2004**, *466*, 114.
(39) Mammeri, F.; Le Bourhis, E.; Rozes, L.; Sanchez, C. *J. Eur. Ceram. Soc.* **2006**, *26*, 259.
(40) Atanacio, A. J.; Latella, B. A.; Barbe, C. J.; Swain, M. V. *Surf. Coat. Technol.* **2005**, *192*, 354.
(41) Oliver, W. C.; Pharr, G. M. *J. Mater. Res.* **1992**, *7*, 1564.
(42) Thünemann, A. F.; Schütt, D.; Kaufner, L.; Pison, U.; Möhwald, H. *Langmuir* **2006**, *22*, 2351.

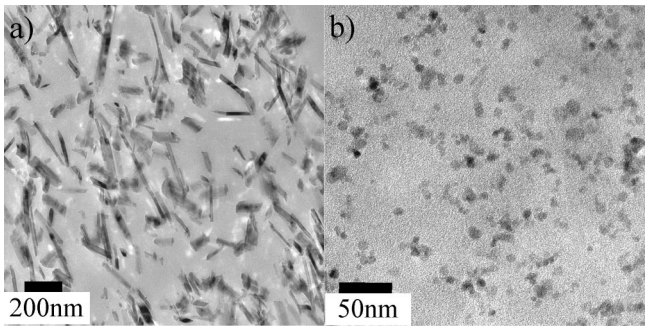

Figure 1. TEM micrographs of (a) a PHEMA–goethite coating with 3.5% volume goethite and (b) a PHEMA–maghemite coating with 1.8% volume maghemite.

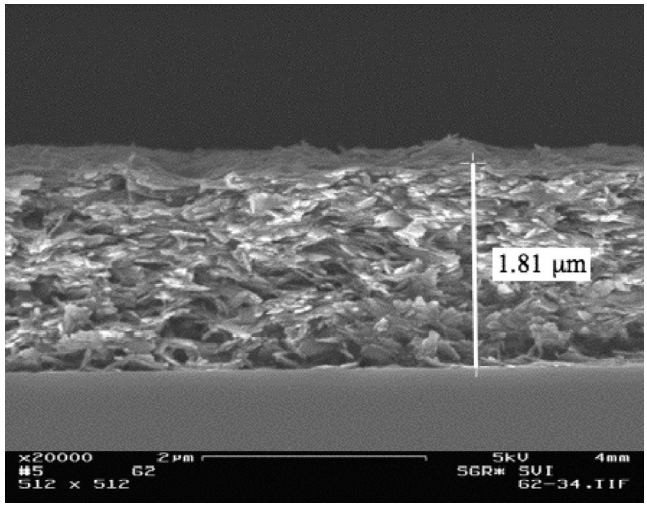

Figure 2. SEM cross-sectional view of the PHEMA–goethite hybrid coating with 3.5% volume goethite showing homogeneous distribution of the goethite nanorods in the film depth.

which allows one to process thick films (>1 μm) depending on both the viscosity of the solutions and the speed during spin coating. This increase in the viscosity of the solutions is faster with goethite than with maghemite nanoparticles and becomes faster at higher temperature. Crack-free, transparent, and homogeneous hybrid coatings with thicknesses greater than 1 μm were prepared. TGA measurements show iron oxide contents comprised between 0 and 10 vol % and 0 and 6 vol % in PHEMA–goethite and PHEMA–maghemite hybrid coatings, respectively.

TEM micrographs of the nanohybrid PHEMA–goethite coating with 3.5% volume iron oxide content (Figure 1a) reveal a uniform dispersion of the particles in the polymer matrix as could be expected from the film transparency. All samples appear free from large aggregates even at high filler contents. Besides, it appears from the SEM cross-sectional micrograph (Figure 2) that the goethite particles are also homogeneously distributed in the depth of the coating. The goethite particles are arranged parallel to the substrate and produce a layered structure.

Figure 3a shows the USAXS-SAXS profiles of goethite particles in the PHEMA matrix obtained on powdered bulk PHEMA–goethite nanocomposites filled with 3.5% and 10% volume contents. The grain size is in average a few tens of micrometers, and they are deposited in a thin layer on kapton sticky tape; the X-ray beam illuminated an area of 2 mm^2

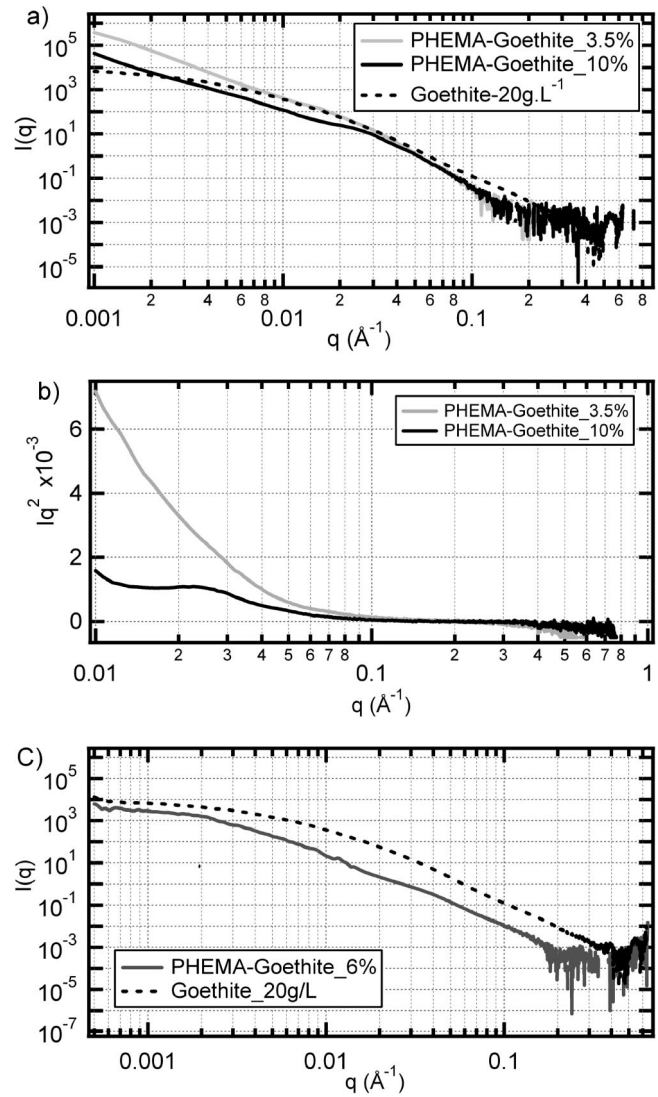

Figure 3. USAXS-SAXS profiles on (a) bulk PHEMA–goethite nanocomposite with 3.5% and 10% volume goethite content, (b) Iq^2 representation on the SAXS range of the bulk PHEMA–goethite nanocomposite with 3.5% and 10% volume goethite content, and (c) USAXS-SAXS profile of goethite nanoparticles obtained on PHEMA–goethite nanohybrid coating filled with 6% volume goethite content and an aqueous suspension of nonaggregated goethite nanorods (dotted line).

and thus the signal makes an average over thousands of grains. The SAXS profile of a diluted goethite aqueous suspension is included as a reference of non-aggregated goethite nanorods (dotted line). The goethite content introduced in the polymer matrix affects significantly the particle SAXS profile in particular at low q-values, with a lower slope observed for the 10% goethite volume content sample. The Iq^2 representation (Figure 3b) further emphasizes these differences, with the occurrence of a shoulder at $q = 0.025$ Å^{-1} and a slope change at lower q-values for the nanocomposite filled with 10% volume goethite content. The shoulder is the signature of a correlation between the goethite rods. In addition, the difference from the dilute solution scattering is stronger at lower q and certainly comes from the scattering of the scrapped grains seen as a whole.[43] In this context, the direct measurement on the hybrid scrapping the film in grains is very useful. Indeed, the USAXS-SAXS profile obtained

on a PHEMA–goethite hybrid coating filled with 6% volume goethite appears more comparable with the profile of the aqueous suspension of non aggregated particles (Figure 3c). This supposes, in agreement with the TEM observations, that the dispersion of the goethite nanoparticles in the PHEMA matrix is homogeneous.

The interactions between polymers and iron oxide particles have been extensively studied.[18,42–49] In particular, iron oxide particles have been reported to interact with polymer matrices through various interaction modes such as hydrogen-bonding,[50] ionic interactions,[42,44] complexation reactions,[45–47,49] or combinations of these different modes. The choice of this system (PHEMA/iron oxide) was governed both by the careful size and shape control of iron oxide nanoparticles offered by "Chimie Douce" synthesis as well as by the ability of iron oxide and PHEMA to interact with each other. Previous works have shown that PHEMA is likely to interact through hydrogen bonding with hydroxyl functional groups at the metal oxide surface[51–53] or through coordination of the carboxyl group to the metal surface atoms.[48,54] Indeed, in the absence of results on the influence of the aspect ratio of iron oxide particles, these interactions turn out to be key parameters governing the mechanical properties of polymer–iron oxide nanocomposites.[18,30,31] Aoyama et al.[31] have introduced Co-modified γ-Fe_2O_3 nanoparticles in vinyl chloride acetate vinyl and vinyl alcohol copolymers of different compositions. They observed an increase of Young's modulus of the magnetic layer with an increase of the hydroxyl-group and carboxy-group concentration in the copolymer. On the contrary, Ciprary et al.[18] have prepared polystyrene, PS, and poly(methyl methacrylate), PMMA γ-Fe_2O_3 nanocomposites. Low interaction strengths were observed with PS but also with PMMA (whereas coordination through Fe surface atom was observed), resulting in a decrease of the Young's modulus with respect to the neat polymers.

The strength of the interactions at the interface between the goethite nanoparticles and the PHEMA matrix has been examined by swelling measurements. Figure 4 shows the evolution of the swelling percentage of the bulk PHEMA–goethite nanocomposites as a function of the goethite volume

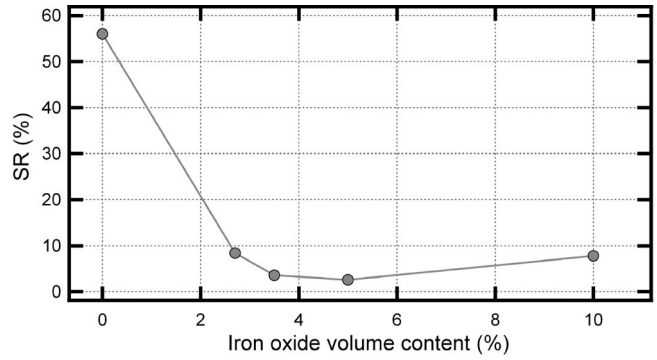

Figure 4. Evolution of the swelling ratio (SR) of PHEMA–goethite determined on bulk nanocomposites in THF versus the goethite volume content.

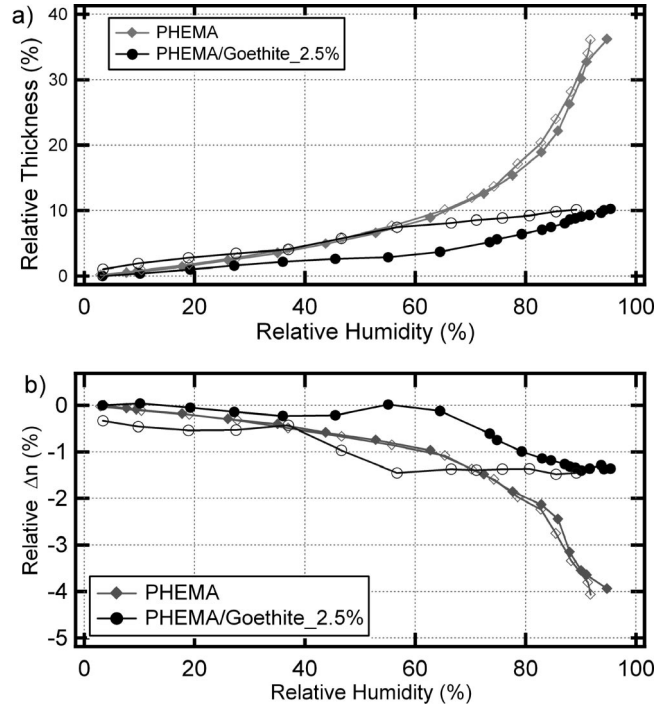

Figure 5. Relative thickness (a) and refractive index (b) of H_2O-swollen PHEMA coatings at 25 °C before and after introduction of 2.5% volume goethite nanoparticles. Filled symbols refer to swelling, and empty symbols refer to deswelling.

content. The introduction of goethite nanoparticles dramatically reduces the swelling of PHEMA in THF. The swelling ratio decreases by a factor of 5 with 2.5% volume goethite content. Minimum swelling occurs between 4% and 5% goethite volume content. A more careful reading reveals a slight increase of the swelling coefficient beyond 5%. This is further emphasized by the ellipsometric measurements as discussed in the next section.

In parallel, specific ellipsometry measurements that allow for the monitoring of the thickness of the coatings as a function of the relative humidity in the measurement cell have been developed to characterize the swelling of the coatings. The method is fast and sensitive, which makes it really relevant for swelling measurements.[55] Figure 5 presents the relative thickness (Figure 5a) and the relative refractive

(43) Spalla, O.; Lyonnard, S.; Testard, F. *J. Appl. Crystallogr.* **2003**, *36*, 338.
(44) Tang, B. Z.; Geng, Y.; Lam, J. W. Y.; Li, B.; Jing, X.; Wang, X.; Wang, F.; Pakhomov, A. B.; Zhang, X. X. *Chem. Mater.* **1999**, *11*, 1581.
(45) McGuire, M. J.; Addai-Mensah, J.; Bremmell, K. E. *J. Colloid Interface Sci.* **2006**, *299*, 547.
(46) Kirwan, L. J.; Fawell, P. D.; Van Bronswijk, W. *Langmuir* **2003**, *19*, 5802.
(47) Kirwan, L. J.; Fawell, P. D.; Van Bronswijk, W. *Langmuir* **2004**, *20*, 4093.
(48) Gong, P.; Yu, J.; Sun, H.; Hong, J.; Zhao, S.; Xu, D.; Yao, S. *J. Appl. Polym. Sci.* **2006**, 1283.
(49) Harris, L. A.; Goff, J. D.; Carmichael, A. Y.; Riffle, J. S.; Harburn, J. J.; St. Pierre, T. G.; Saunders, M. *Chem. Mater.* **2003**, *15*, 1367.
(50) Uner, B.; Ramasubramanian, M. K.; Zauscher, S.; Kadla, J. F. *J. Appl. Polym. Sci.* **2006**, *99*, 3528.
(51) Mohomed, K.; Abourahma, H.; Zaworotko, M. J.; Harmon, J. P. *Chem. Commun.* **2005**, 3277.
(52) Di Maggio, R.; Fambri, L.; Mustarelli, R.; Campostrini, P. R. *Polymer* **2003**, *44*, 7311.
(53) Hajji, P.; David, L.; Gerard, J.-F.; Pascault, J.-P.; Vigier, G. *J. Polym. Sci., Part B: Polym. Phys.* **1999**, *37*, 3172.
(54) Xiang, Y.; Peng, Z.; Chen, D. *Eur. Polym. J.* **2006**, *42*, 2125.
(55) Sirard, S. M.; Green, P. F.; Johnston, K. P. *J. Phys. Chem. B* **2001**, *105*, 766.

index (Figure 5b) determined by ellipsometry on a neat PHEMA coating and a hybrid coating containing 2.5% volume content of goethite nanoparticles, versus the relative humidity (RH) inside the cell. Two different regimes are observed for the PHEMA coating as the relative humidity increases. In a first regime, the stepwise increase of RH induces a moderate raise of the coating thickness while the refractive index slightly decreases until a threshold solvent volume fraction was adsorbed (between 60% and 70% RH). Next begins the second regime where low variations of RH induce a dramatic increase of the coating thickness and a significant drop in refractive index. This regime transition is associated with a glass transition induced by solvent molecules adsorption (SIGT).[56,57]

Similarly to temperature, adsorption of small molecular weight molecules affects the free volume of polymers,[58] inducing a decrease of the glass transition temperature T_g. Keeping the temperature constant, as the relative humidity is increased, water molecules gradually adsorb in the hydrophilic PHEMA polymer until reaching a given solvent volume fraction Φ_g, which lowers the glass transition temperature below room temperature. Beyond Φ_g, the material becomes soft ("rubbery state") and easier to swell. When water is withdrawn during deswelling (decrease of the relative humidity, empty symbols in Figure 5a,b), the evolution of the thickness as well as of the refractive index is very similar to that observed during swelling.

Major changes occur in the presence of goethite nanoparticles. During swelling, the slopes in both regimes are considerably lower. In addition, the deswelling behavior is also affected, thickness and refractive index evolutions present hysteresis loops, while sorption and desorption curves can be superimposed for neat PHEMA. The strong reduction of the coating swelling following the introduction of goethite nanoparticles, in particular in the "rubbery state", as well as the large hysteresis observed during desorption isotherms, reflecting slow chain relaxations, suggests extended interactions between the goethite particles and the PHEMA matrix. It is worth noticing that similar trends with increasing goethite content were observed, using either the traditional weighting method on bulk nanocomposites or ellipsometry on hybrid coatings (Figure 6). Increasing the goethite volume content, a steady drop of the film swelling is observed, which is decreased by a factor of 4 up to 4.5% goethite volume content, before growing up at higher goethite content. Although it is amplified on ellipsometry measurements, this uptake is consistent with the slight increase of the swelling coefficient observed on bulk hybrid materials beyond 4.5% volume goethite content. Because of the difference in solvents (i.e., water vs THF), it is difficult to conclude on an effect of the characterization method or on potentially distinct behaviors between bulk and film materials.

A careful study on the nature of the polymer–particle interactions by FTIR spectroscopy has been carried out.

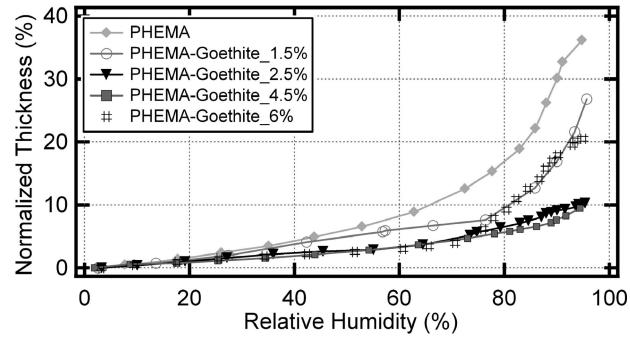

Figure 6. H_2O dilation isotherms at 25 °C for PHEMA–goethite hybrid coatings with various goethite volume content.

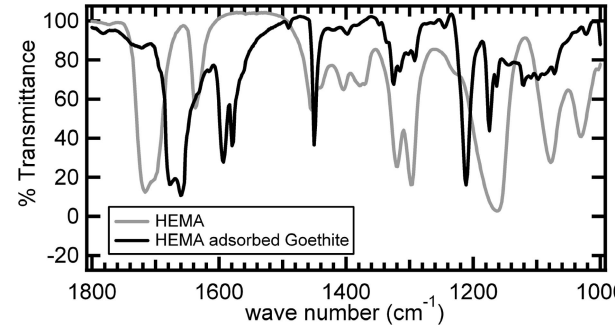

Figure 7. FTIR spectra of HEMA and HEMA-coated goethite nanoparticles.

Figure 7 presents the FTIR spectra obtained on pure HEMA and HEMA-coated goethite nanoparticles. The group assignments of the IR absorption bands for HEMA[59] are summarized in Table 1. The ATR spectrum of the HEMA monomer shows prominent bands at 1716, 1637, 1454, 1162–1078 cm^{-1} attributed to the C═O, C═C, CH_2, and C−O−C vibrations, respectively. Major changes occur upon adsorption at the goethite surface. The C═O stretching is preserved but shifted to lower frequencies and split into a doublet band at 1678 and 1660 cm^{-1}. In addition, the intensities of the bands due to O−C−O asymmetric and symmetric stretching vibrations at 1162 and 1078 cm^{-1}, respectively, which are strong in the pure HEMA spectrum (particularly the former, which is more intense than that due to the C═O stretching vibration), are considerably reduced upon adsorption. Finally, in the HEMA-coated goethite spectrum, the occurrence of spectral bands at 1595−1578 and 1398 cm^{-1} is characteristic of the asymmetric and symmetric stretching vibration frequencies of carboxylate ions, respectively.[59]

These observations indicate that beyond the ability of both PHEMA and goethite particles to interact via hydrogen bonding, other types of interactions also take place. We infer from the FTIR study that, in the presence of goethite nanoparticles, a fraction of ester functions in the monomer HEMA or in PHEMA chains are likely to be hydrolyzed to form carboxylic acid groups.[18] Formation of carboxylic acid groups is explained by the Lewis acid behavior of Fe^{3+} cations, which catalyzes the ester hydrolysis, and in this pH condition, carboxylic acid leads to the complexation at the surface of the nanoparticles of carboxylate groups.

(56) Laschitsch, A.; Bouchard, C.; Habicht, J.; Schimmel, M.; Ru1he, J.; Johannsmann, D. *Macromolecules* **1999**, *32*, 1244.
(57) Wind, J. D.; Sirard, S. M.; Paul, D. R.; Green, P. F.; Johnston, K. P.; Koros, W. J. *Macromolecules* **2003**, *36*, 6433.
(58) Ferry, J. D. *Viscoelastic Properties of Polymers*; Wiley: New York, 1980.
(59) Nakamoto, K. *Infrared and Raman Spectra of Inorganic and Coordination Compounds*, 5th ed.; Wiley: New York, 1997.

Table 1. Spectral Band Assignments for HEMA

vibration	region (cm^{-1})
δ (OH)	1260
δ (CH_2), δ_a (CH_3)	1459
CH_2 twist and rock	1385
νC=C	1637
ν(C=O)	1716
ν_a(C−O−C)	1162
ν(C−O−C)	1078

Table 2. FTIR Peak Assignment for Methacrylic Acid in Solution at pH = 2 and pH =12 and for HEMA after Adsorption at the Goethite Surface

peak position (cm^{-1})			
methacrylic acid solution (pH = 2)	methacrylic acid solution (pH = 12)	HEMA adsorbed	peak assignment
1690		1680−1660	–C=O
1635	1645		–C=C–
	1536	1598–1578	$-COO^-$ (asym)
1454	1455	1454	CH_2
	1414	1398	$-COO^-$ (sym)

The coordination modes (monodentate, bridging bidentate, or chelating bidentate) can be distinguished by infrared spectroscopy with the induced separations between the carboxylate stretch absorption bands ($\Delta\nu$).[45–47,60,61] Table 2 summarizes the peak assignments for methacrylic acid in solution at pH = 2 and pH = 12 and after adsorption at the goethite surface. At pH = 12 in solution, $\Delta\nu$ is 124 cm^{-1}, whereas after adsorption $\Delta\nu$ ranges between 180 and 200 cm^{-1}. Because of the greater value of $\Delta\nu$ as well as the conservation of a strong carbonyl stretching band after adsorption, we assume that after hydrolysis, HEMA coordinates to the goethite surface via a monodentate chelating mode. In addition, the shift of the carbonyl stretching band to lower wavenumbers suggests a weakening of the C=O bond[45] because of hydrogen bonding with the goethite surface.

The complexity of this multicomponent system and the difficulty to get significant responses by Mössbauer or by NMR spectroscopies do not allow an easy estimation of the amount of bounded carboxylate at iron oxide surface particles. According to recent studies on the quantification of the complexation of organic ligands (carboxylate or β-diketonate) grafted onto the surface of non magnetic metal oxide nanoparticles by pulsed field gradient ^{1}H NMR, about 20% of the surface metallic atoms are bounded by capping ligands.[62,63] A similar bounded ligands ratio can be expected for iron oxide-based nanoparticles.

Moreover, the strong absorption of iron oxides in the UV region (particularly goethite)[25] allows for the absorption of a significant amount of photons at the surface of the nanoparticles. This absorption might produce radicals that could initiate the polymerization of monomer adsorbed at the goethite surface.[64,65]

On this basis, the surface interaction between PHEMA and goethite nanoparticles can be represented as shown in Scheme 1.

Surprisingly, in contrast to their widespread use in industry, little data exist in the literature concerning the mechanical properties of iron oxide. The Young's modulus of Fe_2O_3 or Fe_3O_4 ranges from 214 to 350 GPa.[66] However, no reference is made to the influence of the anisotropy of iron oxide crystal. Also, the role of the aspect ratio of iron oxide particles on the mechanical reinforcement of polymer matrix is poorly documented because most of the studies on polymer–iron oxide nanocomposites concern isotropic particles. Gonsalves et al.[67] have reported the incorporation of β-FeOOH acicular nanoparticles in a poly(methyl methacrylate) matrix, but the mechanical properties of the hybrid composites have not been investigated. Figure 8 shows the evolutions of the elastic modulus and hardness of the hybrid coatings versus the goethite content in the nanocomposite materials. Modulus and hardness data are listed in Table 3. Goethite nanoparticles appear as very efficient fillers for the mechanical reinforcement of PHEMA. Both modulus and hardness increase with increasing goethite content until reaching a plateau beyond 5% volume of goethite content ($E \approx 12$ GPa, $H \approx 0.4$ GPa). As compared to the neat PHEMA, modulus (and hardness) has more than doubled from 6% volume goethite loading. It should be further noted that measurements are carried out on a thermoplastic polymer, below its T_g, while mechanical impact of nanoparticles is often recorded for either elastomeric materials or thermoplastic polymer in the rubbery state.

Three main factors are generally considered to discuss the mechanical reinforcement efficiency of inorganic fillers on a polymer matrix: the filler mechanical properties, the filler aspect ratio, and the interactions between the matrix and the filler.[68–70] In this work, the influence of the interactions between the iron oxide fillers and the PHEMA matrix on the mechanical properties of the hybrid coatings is significant. In particular, it is worth noticing that both the Young's modulus (Figure 8a) and the swelling coefficient (Figure 4) follow a similar trend with increasing goethite concentration. In a first step, at low goethite content, the drop in the swelling ratio reflects an increase of the goethite–PHEMA interactions with the amount of the organic−inorganic interface that is directly transcribed into a continuous increase in modulus (and hardness) with the filler content. Next, in a second step, at higher goethite content, the swelling ratio levels off first and then increases slightly while the modulus (and hardness) marks a plateau. The transition occurs for a critical goethite volume fraction Φ_p around 4%. Interestingly, Φ_p also

(60) Mehrotra, R. C.; Bohra, R. *Metal Carboxylates*; Academic Press: New York, 1983.
(61) Dobson, K. D.; McQuillan, A. J. *Spectrochim. Acta, Part A* **1999**, *55*, 1395.
(62) Ribot, F.; Escax, V.; Roiland, C.; Sanchez, C.; Martins, J. C.; Biesemans, M.; Verbruggen, I.; Willem, R. *Chem. Commun.* **2005**, 1019.
(63) Van Lokeren, L.; Maheut, G.; Ribot, F.; Escax, V.; Verbruggen, I.; Sanchez, C.; Martins, J. C.; Biesemans, M.; Willem, R. *Chem.-Eur. J.* **2007**, *13*, 6957.
(64) Soppera, O.; Croutxé-Barghorn, C.; Lougnot, D. J. *New J. Chem.* **2001**, *25*, 1006.
(65) Kramer, S. J.; Mackenzie, J. D. *Mater. Res. Soc. Symp. Proc.* **1994**, *346*, 709.
(66) Samsonov, G. V. *The Oxide Handbook*; IFI/Plenum: New York, 1973.
(67) Gonsalves, K. E.; Li, H.; Santiago, P. *J. Mater. Sci.* **2001**, *36*, 2461.
(68) Sternstein, S. S.; Zhu, A.-J. *Macromolecules* **2002**, *35*, 7262.
(69) Fornes, T. D.; Paul, D. R. *Polymer* **2003**, *44*, 4993.
(70) Sheng, N.; Boyce, M. C.; Parks, D. M.; Rutledge, G. C.; Abes, J. I.; Cohen, R. E. *Polymer* **2004**, *45*, 487.

Scheme 1. Representation of the Hybrid Interface between HEMA and Surface Iron Atoms of Goethite Nanoparticles

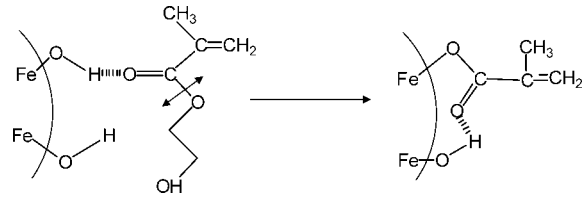

corresponds to modification of the optical properties of the coatings that become birefringent starting from 4% volume goethite content as revealed by optical images under crossed polarization (Figure 9). This indicates that the regime change may result from a structural organization of the goethite nanorods in the PHEMA matrix. This assumption of a self-organization of the goethite nanorods in the PHEMA matrix is further supported by the anisotropy of the SAXS diagram obtained on the birefringent coatings.

Lemaire et al.[71] have shown that a concentrated and stable aqueous dispersion of goethite particles behaves as nematic lyotropic liquid crystals with interesting magnetic properties. The isotropic to nematic transition is governed by the concentration of the goethite particles in the aqueous suspension. We infer that a similar organization of the goethite nanorods may occur after introduction in the HEMA monomer. Lemaire et al.[71]reported a critical volume fraction of goethite of 7% in aqueous suspension, while we observed an earlier transition probably because of the shear stresses induced during the spin-coating process that would further enhance the nanorods organization under long-range radial patterns (Figure 10). As the goethite content increases, the goethite nanorods would first be randomly distributed in the polymer matrix until reaching the critical volume fraction ($\varphi_p = 4\%$) where the particles start to organize. The rod arrangement allows for optimizing their dispersion and as a consequence maximizing their interactions with the HEMA matrix. Beyond that critical point, further increases of goethite volume content lead to the formation of more aggregated structures less favorable in terms of interactions, which level off the mechanical impact of the added particles.

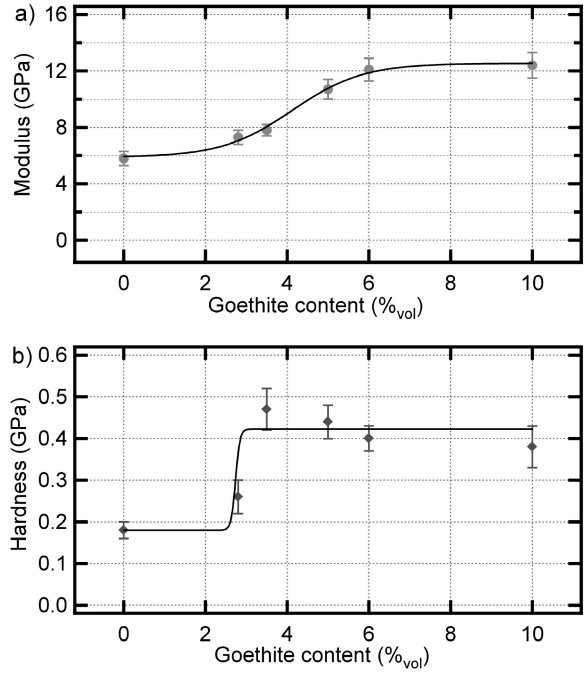

Figure 8. (a) Modulus and (b) hardness of the PHEMA–goethite hybrid coatings as a function of the goethite volume content.

Table 3. Mechanical Characteristics of the PHEMA–Goethite Hybrid Coatings

sample	goethite content (% vol)	aspect	reduced modulus (GPa)	hardness (GPa)
PHEMA	0	transparent	5.8	0.18
PHEMA-G1	0.5	transparent	7.3	0.26
PHEMA-G2	3.5	transparent	7.8	0.47
PHEMA-G3	5	transparent	10.7	0.44
PHEMA-G4	6	transparent	11.8	0.4
PHEMA-G5	10	transparent	12.4	0.38

These observations that emphasize the crucial influence of the interactions between fillers and polymer matrix on the mechanical behavior of the nanohybrid coatings are consistent with the common consideration that the high affinity of polymers to fillers leads to the formation of an adsorbed polymer layer around the particles with specific properties called "interphase"[72] that improves the load transfer between the matrix and the fillers. At the same time, the quality of the particle dispersion throughout the matrix is likely to optimize the amount of interface and to further increase the mechanical reinforcement.

The mechanical response of polymer nanocomposites is usually associated with several interdependent parameters that make difficult to study their respective influences. The versatility of our system allows one to easily replace the anisotropic rod-shaped goethite nanoparticles by isotropic spherical maghemite, keeping a comparable particle dispersion state (Figure 1) and interaction mode with PHEMA (coordination to Fe metal surface atoms through carbonyl functional group after ester hydrolysis). Figure 11 compares the impact of goethite and maghemite volume contents on the Young's modulus of hybrid coatings. Very similar plateau values are reached at high particles content, whereas maghemite spheres present higher mechanical reinforcement at low particle contents. It is worth noticing that not only the shape but also the characteristic size of the particles have been modified. A geometric approach indicates a twice higher particle surface area for maghemite spheres than for goethite nanorods. This suggests that for the same volume fraction of particles the extent of the interphase is higher in the case of PHEMA–maghemite coatings. In particular, this makes the mechanical reinforcement from maghemite particles more

(71) Lemaire, B. J.; Davidson, P.; Ferré, J.; Jamet, J. P.; Panine, P.; Dozo, I.; Jolivet, J. P. *Phys. Rev. Lett.* **2002**, *88*, 125507.
(72) Berriot, J.; Montes, H.; Lequeux, F.; Monnerie, L.; Long, D.; Sotta, P. *J. Non-Cryst. Solids* **2002**, *307*, 310–719.

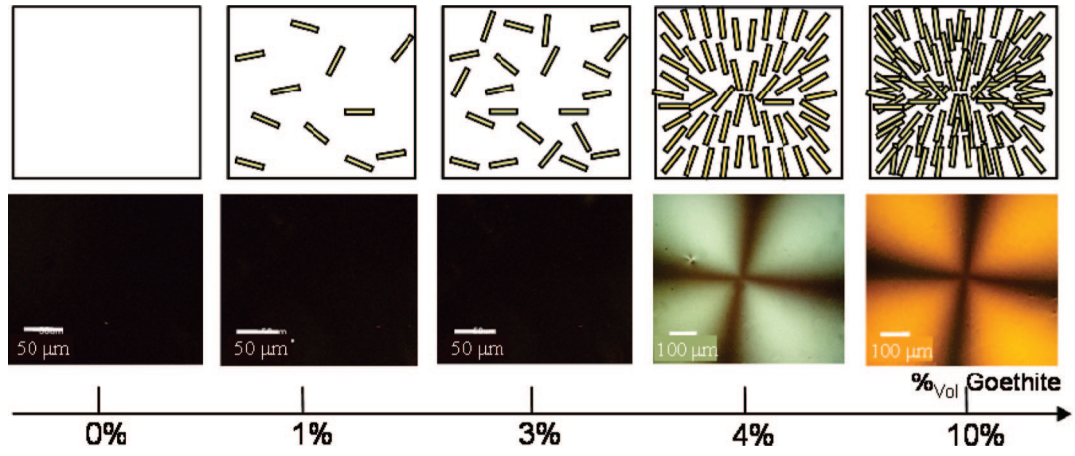

Figure 9. Schematic representation of the reorganization of goethite nanorods and optical microscopy of the coating under cross polarization, induced by the conjugated effects of goethite volume content and shear stresses induced by the spin-coating process.

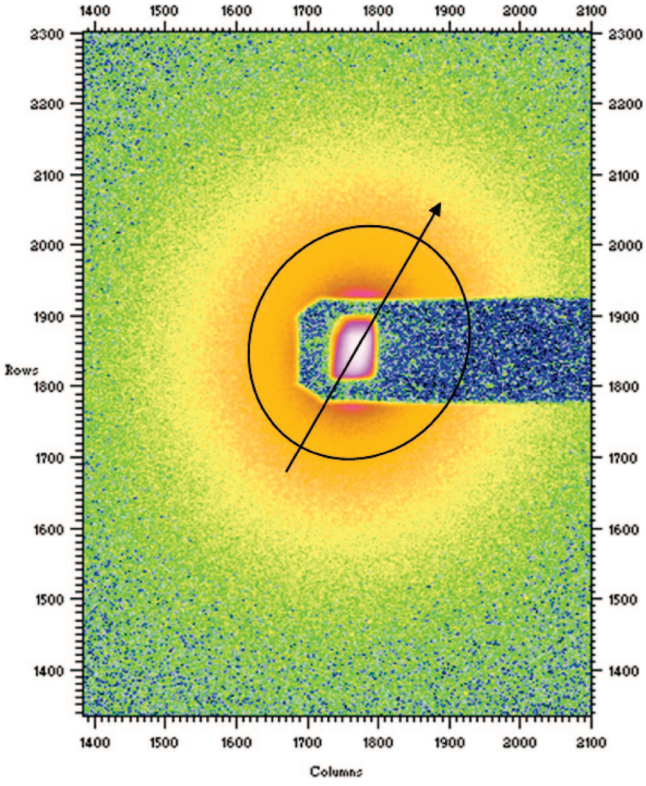

Figure 10. Anisotropic SAXS diagram of a birefringent PHEMA–goethite hybrid coating. The slight anisotropy of the central spot confirms the organization of the goethite nanorods through a radial pattern induced by the spin-coating process.

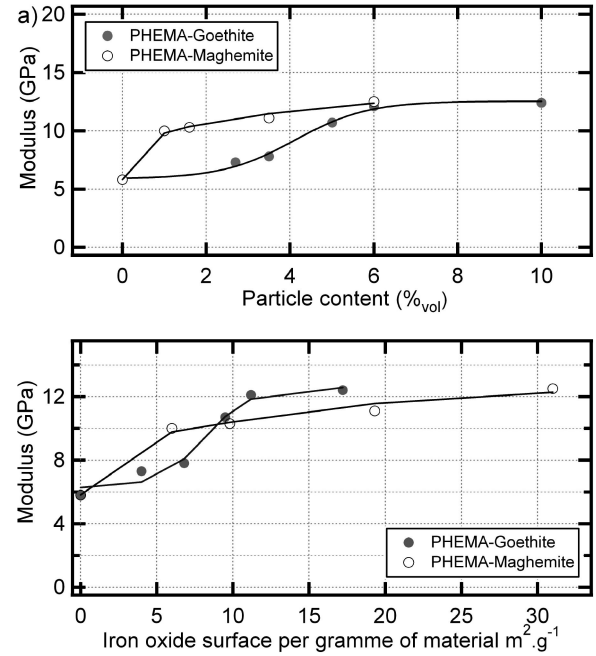

Figure 11. (a) Young's modulus as a function of the particles volume content for PHEMA–goethite (rod-shaped) and PHEMA–maghemite (sphere) nanohybrid coatings. (b) Young's modulus as a function of the corrected surface of interaction between PHEMA and goethite or maghemite particles.

efficient at low particle contents (Figure 11a). At high particle contents, the leveling of the interactions induces similar modulus plateau for both maghemite spheres and goethite nanorods. Figure 11b compares the mechanical reinforcement of PHEMA obtained from goethite and maghemite nanoparticles, taking into account the difference of specific area between both fillers. The Young's modulus of the coatings is displayed as a function of the surface of contact between PHEMA and the iron oxide nanoparticles, assuming a perfect dispersion of the particles and a specific area of 63 $m^2\ g^{-1}$ for goethite and 147 $m^2\ g^{-1}$ for maghemite nanoparticles. From this point of view, both asymmetric rod-shaped goethite nanoparticles and spherical maghemite nanoparticles induce similar mechanical reinforcement of the PHEMA matrix. This suggests that, more than the shape factor that could be mentioned to explain the mechanical reinforcement of polymers from anisotropic fillers, the significant improvement of the mechanical properties, observed through the incorporation of iron oxide particles in a PHEMA matrix, is ruled by the interactions between the particles and the polymer matrix.

Conclusion

Organic−inorganic hybrid nanocomposites coatings, which exhibit photostable color, have been successfully elaborated by incorporating inorganic pigment, goethite nanorods, or spherical maghemite nanoparticles in poly(hydroxyethyl methacrylate) (PHEMA). The mechanical properties of the coatings have been investigated by the nanoindentation

technique. Both goethite nanorods and maghemite nanospheres have proved to yield significant improvement of the mechanical properties of the PHEMA coatings, even at low filler contents. The observed enhancing effect from goethite nanoparticles seems to be correlated with the interfacial structure, the particle dispersion, and the particle morphology. Indeed, we demonstrate that the iron oxide nanoparticles benefit from highly favorable interactions between the polymer chains and the hydroxyl groups present at the nanoparticle surface. While class I^2 hybrid materials through hydrogen bondings between the PHEMA matrix and the goethite particles were expected, the formation of inner coordination complex between iron cation and organic components leads to class II hybrid materials with high mechanical performances.

This study extends the range of fillers available for the mechanical reinforcement of polymer matrix. Provided that one can control the specific interactions between the functional particles and the polymer matrix, the particles are likely to be used not only as a functional element (coloration for example) but also as a reinforcing one, leading to nanocomposites where the polymer acts as binder that fixes the functional nanoparticles while the particles bring the functionality of the hybrid material and participate in the mechanical reinforcement.

In addition to the mechanical enhancement, other specific properties can be expected from the anisotropic nanoparticle. In particular, the optical properties of these new hybrid coatings prove to be especially promising. The goethite-based colored hybrid coatings exhibit via polarized light microscopy birefringent properties. These original optical features are associated with the stabilization inside the organic matrix of a pseudo liquid crystal organization of goethite nanorods. These hybrid complex structures can be considered as crystal liquid analogues, reminiscent of those found in natural hybrid materials.[73,74] This new concept will open a land of promising applications for the design of functional smart coatings.

Acknowledgment. Financial support for the project from Saint-Gobain Research is acknowledged. A. Lelarge and D. Jalabert are gratefully thanked for SEM and TEM images.

CM800253S

(73) Giraud-Guille, M. M. *Int. Rev. Cytol.* **1996**, *166*, 59.
(74) Sanchez, C.; Arribart, H.; Giraud-Guille, M. M. *Nat. Mater.* **2005**, *4*, 277.